

Adjustable Functionalization of Hyper-Cross-Linked Polymers of Intrinsic Microporosity for Enhanced CO₂ Adsorption and Selectivity over N₂ and CH₄

Haoli Zhou, Christopher Rayer, Ariana R. Antonangelo, Natasha Hawkins, and Mariolino Carta*



Cite This: <https://doi.org/10.1021/acsami.2c02604>



Read Online

ACCESS |



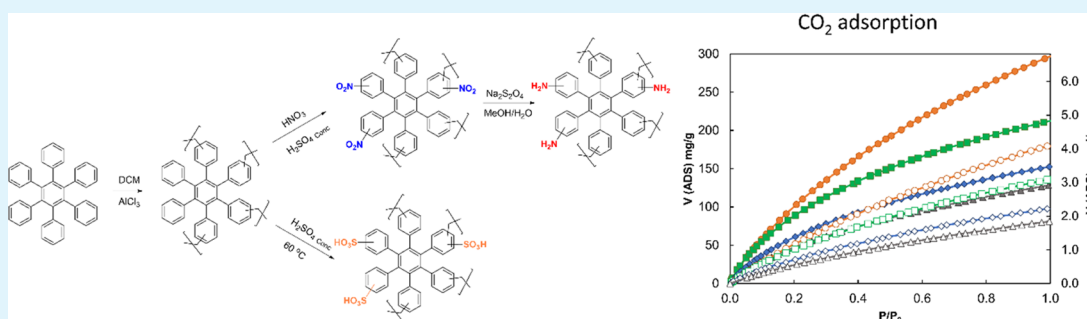
Metrics & More



Article Recommendations



Supporting Information



ABSTRACT: In this paper, we report the design, synthesis, and characterization of a series of hyper-cross-linked polymers of intrinsic microporosity (PIMs), with high CO₂ uptake and good CO₂/N₂ and CO₂/CH₄ selectivity, which makes them competitive for carbon capture and biogas upgrading. The starting hydrocarbon polymers' backbones were functionalized with groups such as -NO₂, -NH₂, and -HSO₃, with the aim of tuning their adsorption selectivity toward CO₂ over nitrogen and methane. This led to a significant improvement in the performance in the potential separation of these gases. All polymers were characterized via Fourier transform infrared (FTIR) spectroscopy and ¹³C solid-state NMR to confirm their molecular structures and isothermal gas adsorption to assess their porosity, pore size distribution, and selectivity. The insertion of the functional groups resulted in an overall decrease in the porosity of the starting polymers, which was compensated with an improvement in the final CO₂ uptake and selectivity over the chosen gases. The best uptakes were achieved with the sulfonated polymers, which reached up to 298 mg g⁻¹ (6.77 mmol g⁻¹), whereas the best CO₂/N₂ selectivities were recorded by the aminated polymers, which reached 26.5. Regarding CH₄, the most interesting selectivities over CO₂ were also obtained with the aminated PIMs, with values up to 8.6. The reason for the improvements was ascribed to a synergetic contribution of porosity, choice of the functional group, and optimal isosteric heat of adsorption of the materials.

KEYWORDS: polymers of intrinsic microporosity, isothermal gas adsorption, pore size distribution, selectivity, isosteric heat

INTRODUCTION

Carbon dioxide is accepted as being the most dominant contributor to global warming.¹ According to a recent report from NASA,² the concentration of CO₂ in the atmosphere recorded to date (last data from 2021) is greater than at any other time in modern history, exceeding 417 ppm and rising. This roughly translates into a ~49% increase since the beginning of the industrial age (280 ppm in ~1850) and a 13% increase since 2000, when it was already close to 370 ppm. It is widely recognized that we are at its highest point in over 20,000 years, as it is calculated that the concentration of CO₂ at the end of the last glacial age was ~185 ppm. There is also an overwhelming scientific consensus (18 of the best recognized scientific associations) that the steep increase in the concentration is largely attributable to human activities.³

Sensibly, governments, industries, and academia started addressing the problem a long time ago, implementing new policies aimed at reducing the release of this greenhouse gas into the environment via new carbon capture and sequestration schemes (CCS).⁴ Various systems have been developed to either retrofit existing chemical plants, with modules intended to trap CO₂ before it is released into the atmosphere (postcombustion carbon capture, the most common) or by removing it once already released via direct air carbon capture

Received: February 11, 2022

Accepted: April 13, 2022

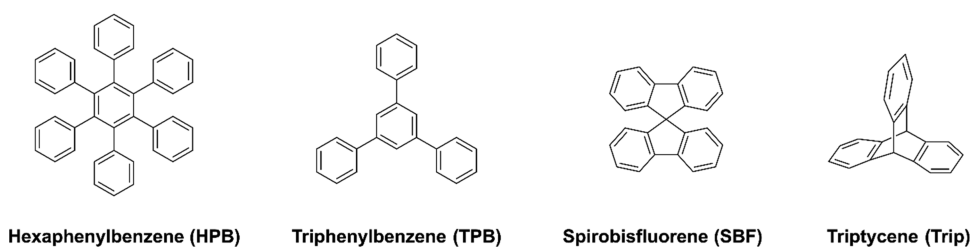


Figure 1. Monomers used in this work to prepare the hydrocarbon-based hyper-cross-linked PIMs.

(DACCS).^{5,6} The latter is a fascinating option but it is also very difficult to be accomplished, as the concentration of CO₂ in the air is extremely low for current techniques (just over 400 ppm).⁷ The former is certainly more feasible for the industry, for instance, by loading a variety of adsorbents in pre-existing plants and capturing CO₂ via temperature (TSA),⁸ pressure (PSA),⁹ or vacuum swing (VSA)¹⁰ adsorption. The overall operating costs of these techniques are regarded as cheaper than the typical amine-bed carbon capture.¹¹ In fact, to date, the removal of CO₂ from flue gas is mainly achieved by its absorption onto aqueous amine solutions, mainly due to their affinity for slightly Lewis-acid gases like CO₂. However, the energy penalty of their utilization is strongly affected by the high isosteric heat of adsorption (Q_{st}) of CO₂, which means that its desorption after capture is very energy-demanding, and that makes the amine beds difficult to be regenerated.¹² Researchers suggest Q_{st} values of about 50 kJ mol⁻¹ to define the boundary between chemisorption, where a chemical bond with the gas and the sorbent is achieved, and physisorption, where the gas is simply “mechanically” trapped within pores (the energy of physisorption is comparable to van der Waals (vdW) forces).¹³ This definition is not conclusive, anyway, as several parameters need to be considered at the same time to have a full picture.¹⁴ The general conclusion is that, if the gas can diffuse rapidly within the pores, a high Q_{st} guarantees a quick CO₂ capture but it also requires more energy for its desorption, whereas a low Q_{st} grants a quick release but more adsorption cycles are necessary to achieve an acceptable removal performance. It is evident that a good compromise between the two will produce an ideal material for carbon capture. This means that low/medium Q_{st} (between 20 and 35 kJ mol⁻¹, so still in the physisorption range) are desirable for carbon capture, preferentially via PSA or VSA.¹⁵ This could be accomplished by producing highly porous materials (so, promoting physisorption) and decorating them with functional groups that enhance their affinity for CO₂ (i.e., keeping the chemisorption to acceptable values). As a good example of such a compromise, trapping CO₂ using ionic liquids (ILs) represents an emerging CCS technique. ILs are often embedded in porous materials to combine the advantages provided by their low vapor pressure, tunable structures, and the presence of a permanent charge that increases their capability to trap CO₂ efficiently. In addition, the porosity of the support maximizes the contact of the gas within their structures.¹⁶ For this reason, it is not uncommon to see IL composite systems for CO₂ capture blended with metal-organic frameworks (MOFs)¹⁷ or other porous polymeric systems.^{18–20} Porous materials such as MOFs seem, in fact, very attractive for CCS²¹ because of their high surface areas and the tunability of their structures that allows the introduction of functional groups. However, the coordinated metals enclosed in their backbones make them less attractive

from the environmental point of view. Insoluble amorphous materials, such as hyper-cross-linked polymers, are a valid alternative to MOFs, especially considering their metal-free structures. To be competitive for carbon capture, the working capacity of these sorbents should result in greater than 2 mmol g⁻¹ (>88 mg g⁻¹) at 298 K, they should be very stable and resistant for numerous cycles and, of course, inexpensive and producible on large scale.¹⁵ Several porous hyper-cross-linked polymers have been investigated for this purpose, and the best performances were achieved when functional groups such as hydroxy (–OH),^{22,23} amino (–NH₂),^{24–26} nitro (–NO₂),²⁷ and sulfonic (–SO₃H)^{28,29} were incorporated in the backbone, which improved the affinity of the material for CO₂.

Polymers of intrinsic microporosity (PIMs) represent an emerging family of porous polymers. They are materials in which porosity originates from the appropriate choice of the monomers, which leads to an inefficient packing of the polymer chains in the solid state and to the formation of voids of nanodimension.³⁰ They have proved to be excellent in separating CO₂ from other gases due to a combination of a narrow pore size, which leads to excellent molecular sieving properties, and high solubility of CO₂ in their backbones.^{31–33}

In fact, they typically exhibit pore sizes between 3.5 and 8.5 Å³⁴ so that CO₂, which has a kinetic diameter of 3.3 Å, can interact with both sidewalls of the pores.³⁵ However, the main advantage of PIMs probably lies in the ease of their synthesis and functionalization, which consents to introduce polar groups that improve the affinity for CO₂.³⁶ Recently, the synthesis of a series of new hyper-cross-linked PIMs with very high Brunauer–Emmett–Teller (BET) surface areas (SA_{BET} up to 2435 m² g⁻¹) was reported by Msayib and McKeown.³⁷ They are prepared from hydrocarbon monomers and polymerized via a simple and efficient Friedel–Crafts reaction.

The great potential of these knitted polymers and the simplicity of the reaction was further demonstrated by Lau et al., who reported the synthesis of a triptycene hyper-cross-linked PIM via flow chemistry, also proving the possible scalability of the method.³⁸ In a recent work, we reported the functionalization of two of these PIMs with sulfonic groups, which proved very effective in selectively removing anti-depressants from wastewater.³⁹

In this paper, we used the same approach systematically synthesizing and functionalizing a series of hydrocarbon-based PIMs, namely hexaphenylbenzene (HPB), triphenylbenzene (TPB), spirobisfluorene (SBF), and triptycene (Tript), with amino (–NH₂), nitro (–NO₂), and sulfonic groups (–SO₃H), focusing the study on the assessment of their CO₂ uptake and their selectivity against N₂ and CH₄ to elucidate their potential for CCS and biogas upgrading.

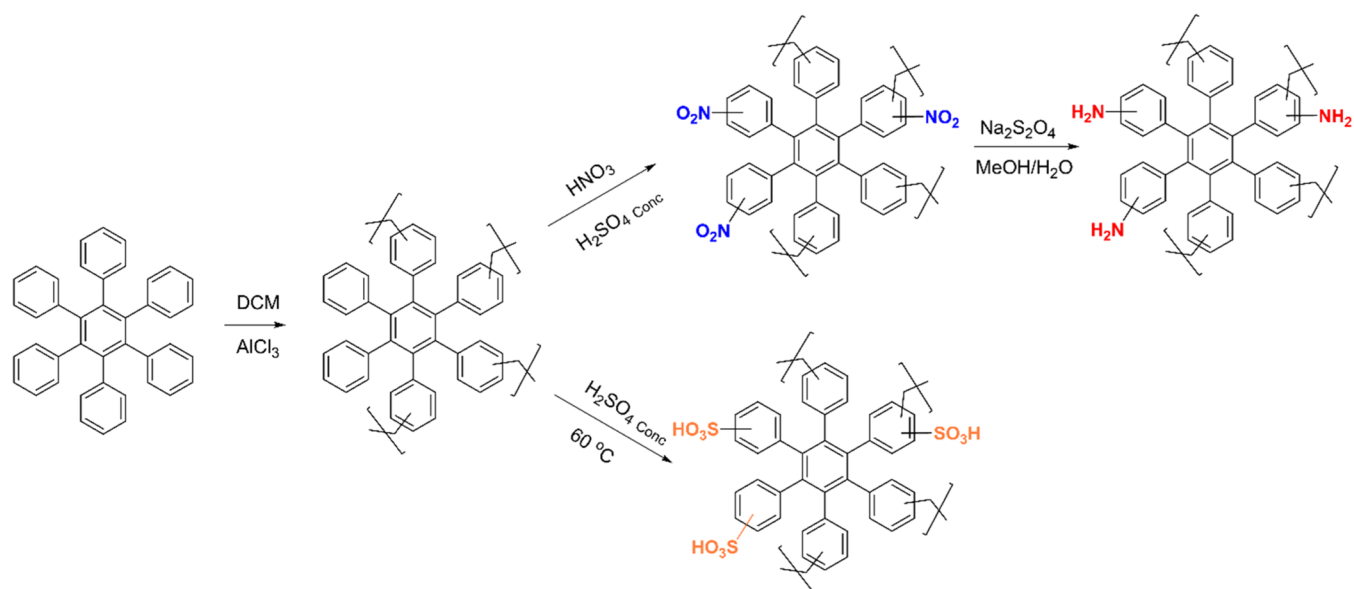


Figure 2. Synthesis and postpolymerization modification of HPB-PIM.

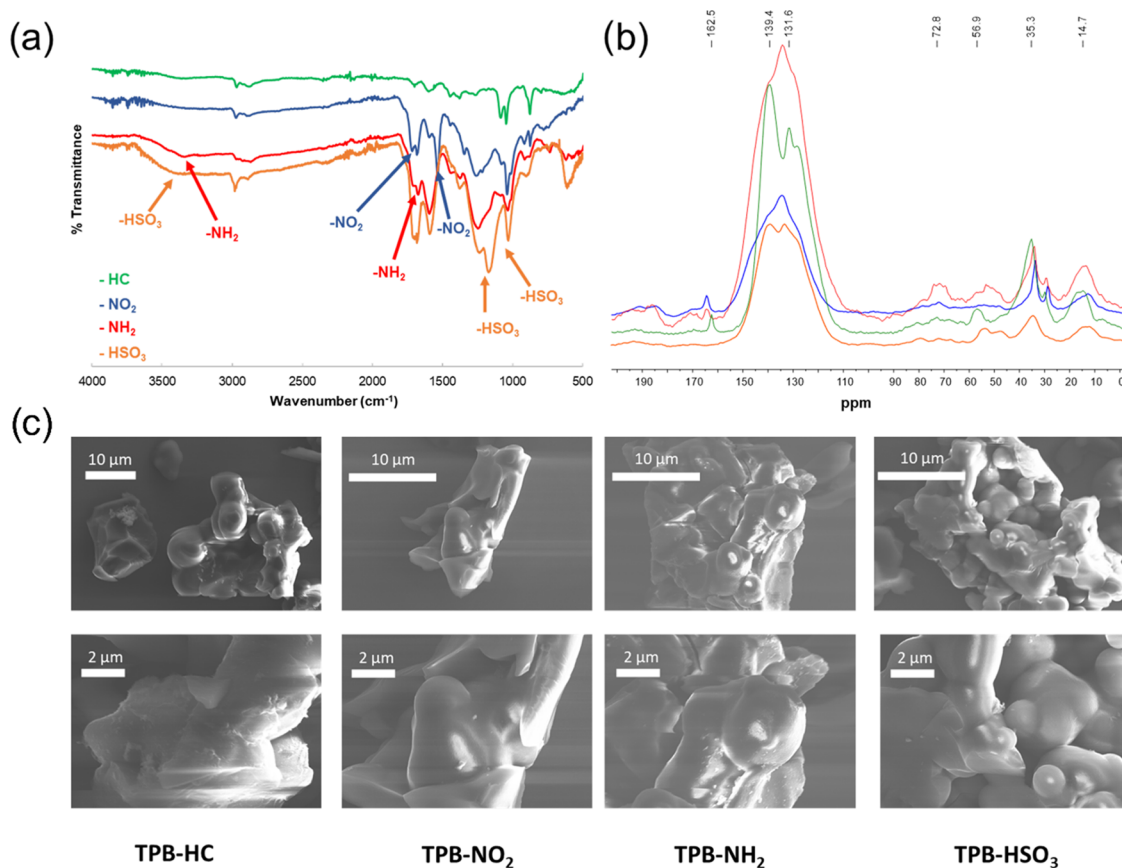


Figure 3. (a) FTIR, (b) ^{13}C SSNMR, and (c) SEM images of TPB-PIMs.

RESULTS AND DISCUSSION

Synthesis and Functionalization of Polymers. The synthesis of the hydrocarbon hyper-cross-linked polymers was performed following the procedure reported by Msayib and McKeown.³⁷ The reaction consists of a Friedel–Crafts polymerization of the monomers, catalyzed by AlCl_3 in the presence of dichloromethane (DCM), which acts as both the solvent and as a cross-linker bidentate ligand.

We chose to use only monomers known to induce high BET surface areas (SA_{BET}) in the final material (Figure 1). Starting from a high microporosity is crucial, especially considering that the introduction of functional groups in the preformed backbone may cause the loss of some of it due to a known “pore filling” effect.^{40,41} So, if we want to retain some of the original internal free volume (IFV), which is deemed necessary to improve the gas separation performance by molecular

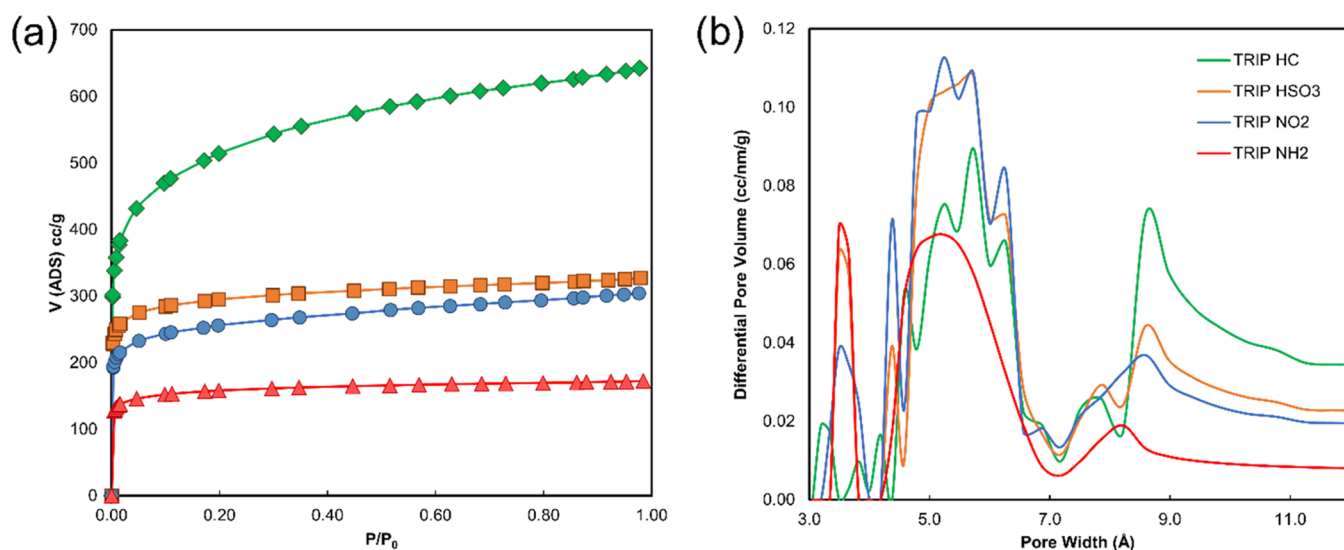


Figure 4. (a) Overlay of N₂ adsorption isotherms (77 K) and (b) NLDFT pore size distribution calculation (from CO₂ adsorption at 273 K) for PIM-TRIP polymers. Desorption curves were removed for clarity.

sieving, it is essential to start from materials with a very high surface area. As anticipated, despite the loss of porosity, we trusted that the addition of polar groups would enhance the affinity of the material for CO₂, with an improvement in the selectivity toward larger gases such as N₂ and CH₄.^{42,43} The fastest way to introduce such groups is by inserting them via postpolymerization modifications of their aromatic structures. For instance, we thought to incorporate either the basic amines (via nitration, followed by their reduction)⁴⁴ or acidic groups via direct sulfonation.³⁹ In a recent paper, we reported the successful addition of sulfonic groups to two hyper-cross-linked hydrocarbon polymers (TPB and TRIP) by simply reacting the preformed backbone with concentrated sulfuric acid at 60 °C and obtaining an average of three acid groups per repeated units, as proven by acid/base titration.^{39,45} The same procedure was herein used to also sulfonate the SBF and HPB polymers. The introduction of the basic functionalities was achieved by nitration of the aromatic moieties with HNO₃ catalyzed by H₂SO₄, followed by the reduction of the nitro groups with Na₂S₂O₄ in a mixture of alcohol/water. Figure 2 shows the scheme of a typical procedure, in this case, using HPB as an example of the hydrocarbon backbone. All of the reported polymers produced similar results in terms of both yields and purity, which proves the validity and reproducibility of our protocols. Details about the synthesis for all of the polymers are reported in the Supporting Information (SI).

Structural Characterization of the Functionalized Polymers. As expected from the type of polymerization, all of the synthesized hyper-cross-linked PIMs were found completely insoluble in common organic solvents, which prevented their characterization via the typical solution-based techniques, i.e., ¹H NMR, needed for confirmation of the composition of the backbone, or gel permeation chromatography (GPC), typically used for the estimation of the molecular mass of the chains. The carbon contents could be, in theory, determined by elemental analysis but they were always proved lower than the expected one. This is something that is frequently observed in highly porous aromatic polymers where water molecules and other adsorbed gas may change the ratios, which makes this technique poorly reproducible.^{46–48} The correct composition was demonstrated by Fourier

transform infrared (FTIR) spectroscopy and solid-state ¹³C NMR (SSNMR), which proved the efficient incorporation of the different functional groups. As an example, Figure 3a shows the overlay of the FTIR spectra of the TPB-PIMs. The bands around 3300 and 1550 cm⁻¹ confirm the presence of the –NH₂ groups on the aminated materials, whereas peaks centered at ~3450, ~1200, and ~1000 cm⁻¹ show the typical signatures of the –HSO₃ groups of the sulfonated version. The FTIR of the nitrated TPB polymer is very similar to the aminated version, apart from the obvious lack of –NH₂ peaks. Figure 3b shows the overlay of the ¹³C SSNMR of the same TPB polymers, which was used to further validate the correct structure of the hyper-cross-linked PIMs.

As expected, the broad peak in the area around 160 and 130 ppm confirms the presence of aromatic carbons, and several smaller peaks, in the range between 75 and 15 ppm, suggest the presence of the methylene cross-linkers, some of which likely shifted due to the vicinity of a polar functional group. FTIR and ¹³C SSNMR spectra for all of the other single polymers are shown in the SI (Figure SI12–15 for FTIR and Figure SI16–31 for ¹³C SSNMR). Scanning electron microscopy (SEM) images (Figure 3c) were taken to investigate potential changes in the morphology of the material due to the insertion of different functionalities. The analysis of the images at different magnifications supports the formation of amorphous materials very similar to one another. In fact, apart from TPB-HC, which seems to exhibit a slightly larger particle size than the other three, all polymers seem to display globular particles of around 1–2 μm in size. All of the other functionalized polymers herein reported followed the same trend indicated by TPB-PIMs, which is also in line with similar published materials,^{29,49,50} proving the reproducibility of our methods.

Physical Characterization. The measurement of the microporosity was performed via the typical isothermal N₂ adsorption at 77 K, with the calculation of the individual apparent BET surface areas (SA_{BET}). All of the hydrocarbon-based PIMs proved to be highly microporous, with a type I(a) isotherm that denotes a steep uptake at low partial pressure, typical of ultramicroporous polymers. The lack of a pronounced hysteresis (Figures SI3, SI7, SI5, and SI9) hints

Table 1. Physical Characterization of Polymers and Gas Selectivity

Polymer	BET (m ² g ⁻¹)	Pore volume ^a (cc g ⁻¹)	CO ₂ adsorption		IAST selectivity ^b		Q _{st} ^c (KJ mol ⁻¹)
			273 K (1 bar) (mg g ⁻¹) (mmol g ⁻¹)	298 K (1 bar) (mg g ⁻¹) (mmol g ⁻¹)	CO ₂ /N ₂	CH ₄ /CO ₂	
This Work							
Hydrocarbon							
PIM-HPB	1933	1.63	137 (3.12)	69 (1.57)	13.5		21.6
PIM-SBF	1604	0.837	144 (3.28)	79 (1.79)	11.4		23.3
PIM-TPB	2540	1.300	220 (5.00)	121 (2.75)	14.1	3.1	25.2
PIM-Tript	1880	0.996	166 (3.78)	109 (1.48)	13.9	3.6	24.2
Nitrated							
PIM-HPB-NO ₂	1286	1.24	137 (3.11)	88 (2.00)	26.5	7.1	29.5
PIM-SBF-NO ₂	909	0.57	147 (3.34)	98 (2.23)	23.4	6.8	30.1
PIM-TPB-NO ₂	950	0.553	225 (5.13)	137 (3.11)	24.7	8.0	32.1
PIM-Tript-NO ₂	975	0.472	214 (4.87)	115 (2.61)	24.8	6.8	34.5
Aminated							
PIM-HPB-NH ₂	997	0.969	123 (2.80)	81 (1.84)	21.6	7.0	30.4
PIM-SBF-NH ₂	669	0.303	128 (2.90)	97 (2.20)	24.2	6.3	27.7
PIM-TPB-NH ₂	710	0.333	196 (4.45)	131 (2.98)	26.1	8.6	31.7
PIM-Tript-NH ₂	610	0.270	157 (3.57)	124 (2.81)	25.5	7.4	34.7
Sulfonated							
PIM-HPB-HSO ₃	1390	1.31	128 (2.9)	81 (1.84)	18.7	7.1	27.9
PIM-SBF-HSO ₃	1063	0.557	152 (3.45)	98 (2.23)	23.4	6.4	28.7
PIM-TPB-HSO ₃	1585	0.852	298 (6.77)	179 (4.07)	17.9	7.8	29.0
PIM-Tript-HSO ₃	1145	0.507	216 (4.91)	135 (3.07)	19.2	7.8	30.9
Comparison with Other Polymers							
Ad-MALP-1 ²⁵	1629	0.396	182	89	28.4	5.37	26.7
Ad-MALP-4 ²⁵	1541	0.384	166	78	25.4	4.21	27.4
PI-ADNT ²⁷	774	0.415	150	85	25	9	35
PI-NO ₂ -1 ²⁷	286	0.155	177	89	18	11	43
TPPA-DMB ⁶⁴	883	0.53	124	76	25	5.3	
TATHCP ⁶⁵	997	0.63	125	77	22	4.8	33
NPC-700-KOH ⁶⁶	2616	1.14	240	127	21.5		24
HCP2a-K700 ⁶⁷	1964	1.04	251	134	10.8		24.8
PBZC-3-900 ⁶⁸	2423	1.47	359	204	31	6.2	35
Polymer 3 ⁶⁹	1717	0.37	188	103	19.4	4.1	26.5
NPOF-1-NO ₂ ⁴⁴	1295	0.36	160	111	20	6	29.2
NPOF-1-NH ₂ ⁴⁴	1535	0.48	250	166	25	10	32.1
HCP-SC-SO ₃ H	1246	0.94		62	19		35
C1M3-Al ⁷⁰	1783	1.29	181		23.4		20.1

^aAt $P/P_0 \sim 0.98$. ^bCalculated according to IAST at 298 K and 1 bar.^{59,60} ^cIsosteric heat of adsorption (in kJ mol⁻¹) of corresponding gas at zero coverage calculated from isotherms collected at 273 and 298 K and fitted with the Langmuir–Freundlich equation and calculated via the Clausius Clapeyron equation.

at small and interconnected pores similar to microporous carbons.⁵¹ The SA_{BET} ranges from TPB (2540 m² g⁻¹) > HPB (1933 m² g⁻¹) > TRIP (1880 m² g⁻¹) > SBF (1604 m² g⁻¹), which is similar to the ones previously reported by Msayib and McKeown.³⁷ Figure 4a shows the overlay of the N₂ adsorption isotherms for the PIM-TRIP family.

The pore size distribution analysis, calculated via nonlocal density functional theory (NLDFT) from the CO₂ adsorption at 273 K, provided values in the typical range of PIMs. The first set of pores centered around 3.5 Å confirmed the ultramicroporosity of these materials, followed by two more peaks centered around 5.6 and 8.6 Å. Despite the fact that pore size distribution (PSD) assessed via gas adsorption is known to be mostly qualitative,⁵² it is worth noting that the contribution coming from the larger peak (8.6 Å) is more evident for the pure hydrocarbon polymers and decreases for the functionalized ones (TRIP-PIMs in Figure 4b). This suggests that the substitution leads to a general shrinking of the pores that

move, predominantly, toward the ultramicroporous region. This feature is very important for the understanding of the separation of CO₂ from N₂ and CH₄, as it will not be dominated only by the enhanced affinity due to the introduction of substituents, but also by an improved molecular sieving effect. The physical data for all polymers are shown in Table 1, whereas the single isotherms and the pore size distribution (PSD) are reported in the SI (Figure SI3–10). The postpolymerization modifications led to the expected loss of porosity, but not all of the functionalities had the same impact. In fact, both nitro- and sulfonic-containing polymers retained a good amount of the initial porosity, with PIM-NO₂ ranging from 909 to 1286 m² g⁻¹ and PIM-HSO₃ from 1145 to 1390 m² g⁻¹. This suggests that the introduction of such groups leads to the loss of some of the internal free volume but, apart from the expected pore-filling effect, there are no other contributing factors that reduce the overall porosity. PIM-NH₂, on the other hand, provided lower SA_{BET}

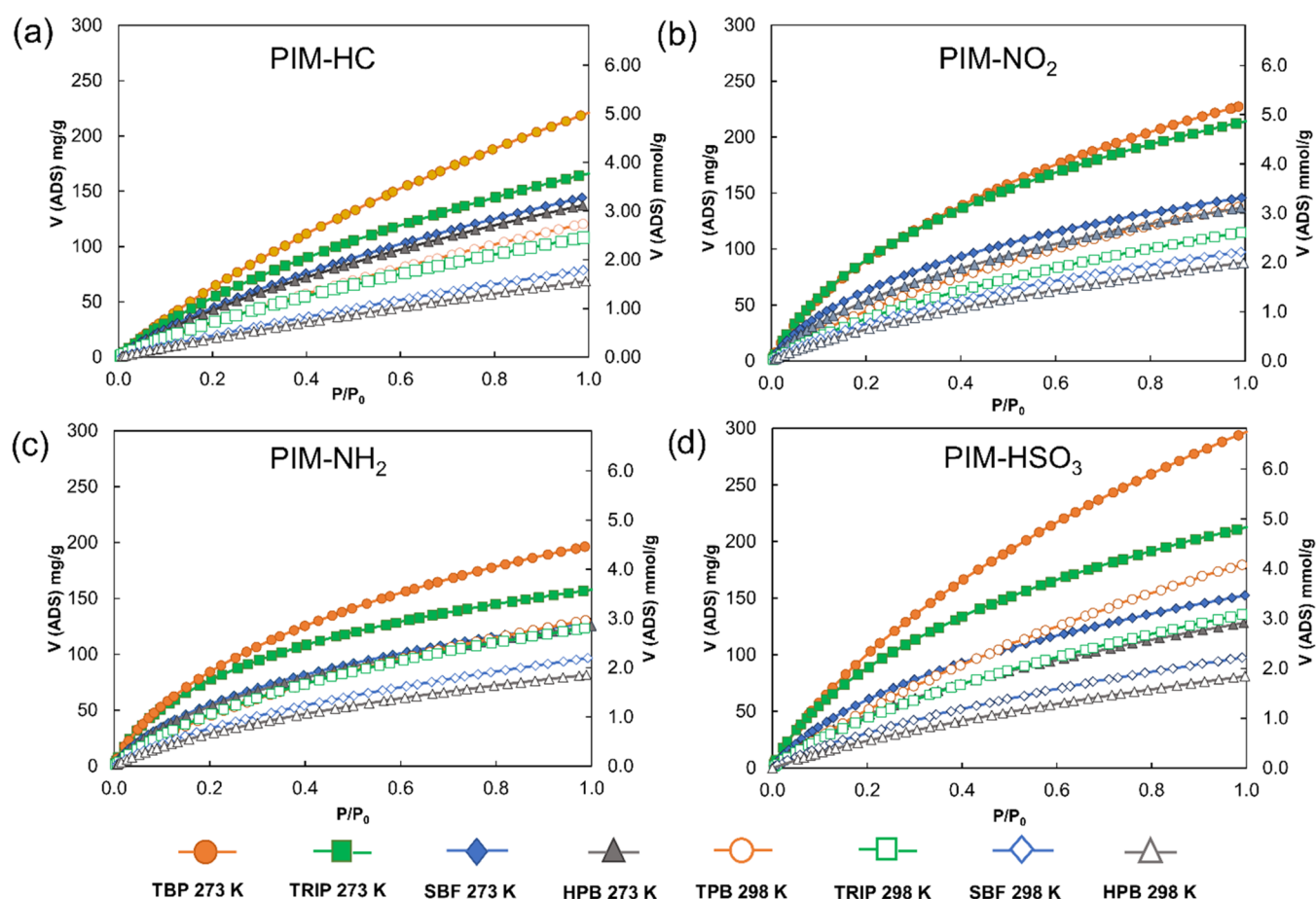


Figure 5. CO₂ adsorption of hyper-cross-linked PIMs at 273 and 298 K.

values, ranging from 610 to 997 m² g⁻¹, showing a more pronounced loss of porosity compared to the other two families of substituted PIMs. This behavior is not uncommon for aminated porous polymers^{24,44,53} and suggests that the presence of amines affects the overall porosity more than other groups, most likely promoting stronger intermolecular hydrogen bonding that pulls the polymer chains closer together.⁵⁴

CO₂ Adsorption. The CO₂ uptake was strongly influenced by the incorporation of functional groups, which altered uptakes and selectivity in the way we expected. From Table 1 and Figure 5, we can see that the CO₂ uptake at 273 K for all of the hydrocarbon-based PIMs is very high, as the best polymer (PIM-TPB) adsorbed 220 mg g⁻¹ (5.00 mmol g⁻¹) of CO₂ at 1 bar, followed by PIM-TRIP > PIM-SBF > PIM-HPB. The excellent adsorption was attributed to the very high porosity of the PIMs. Despite producing lower surface areas, the functionalization generated high CO₂ uptakes for the nitro- and amino-containing PIMs, demonstrating the benefits of having such groups in the backbone, which showed a further improvement after the sulfonation process. PIM-TPB-HSO₃, in fact, proved the best of the entire set with a remarkable CO₂ uptake of 298 mg g⁻¹ (6.77 mmol g⁻¹) at 273 K and 179 mg g⁻¹ (4.06 mmol g⁻¹) at 298 K, which makes it competitive with some of the state-of-the-art polymers reported, for comparison, at the bottom of Table 1. All of the reported PIMs showed the same trends, with the sulfonated polymers providing better uptakes than the nitrated, which proved to be slightly better than the aminated versions. The latter came as a surprise as more basic moieties were thought to have a better affinity for

CO₂, which is a weak Lewis acid, but the reduced porosity probably compensated for the higher affinity, reducing the overall performance. The reproducibility of the work clearly shows that the sulfonated and nitrated PIMs are superior, at least in the absence of water/moisture in the adsorbed gas.

Selectivity Studies. The selectivity of CO₂ over other gases is undoubtedly as important as the final uptakes, especially when the materials are designed to separate potential mixtures. It is known that removing CO₂ from any gases is crucial to assessing the performance of the adsorbent materials for carbon capture and sequestration (CCS). The removal of CO₂ from methane, instead, is an important industrial process, aimed to improve the performance of natural gases when used as fuels (also known as biogas upgrading).^{55,56}

All of the studies were conducted by measuring the adsorption of single gases at 298 K and taking the selectivity at 1 bar, so mimicking vacuum swing adsorption conditions (VSA).^{57,58} The potential mixture of the two gases was set at 15/85 for CO₂/N₂ or 50/50 CO₂/CH₄, using the IAST method to assess the potential separation^{59,60} and simulating the VSA conditions for postcombustion carbon capture and the biogas upgrading. All hydrocarbon polymers proved to be poorly selective toward both N₂ and CH₄. This is not unexpected, as the hydrocarbon backbone is rather inert, and we saw that the pores seem slightly larger compared with the substituted versions. As shown in Table 1, despite the relatively lower uptakes, both nitrated and aminated polymers showed better selectivities than sulfonated ones, with CO₂/N₂ values ranging from 23.4 to 26.5 (Figure 6a). The CO₂/CH₄

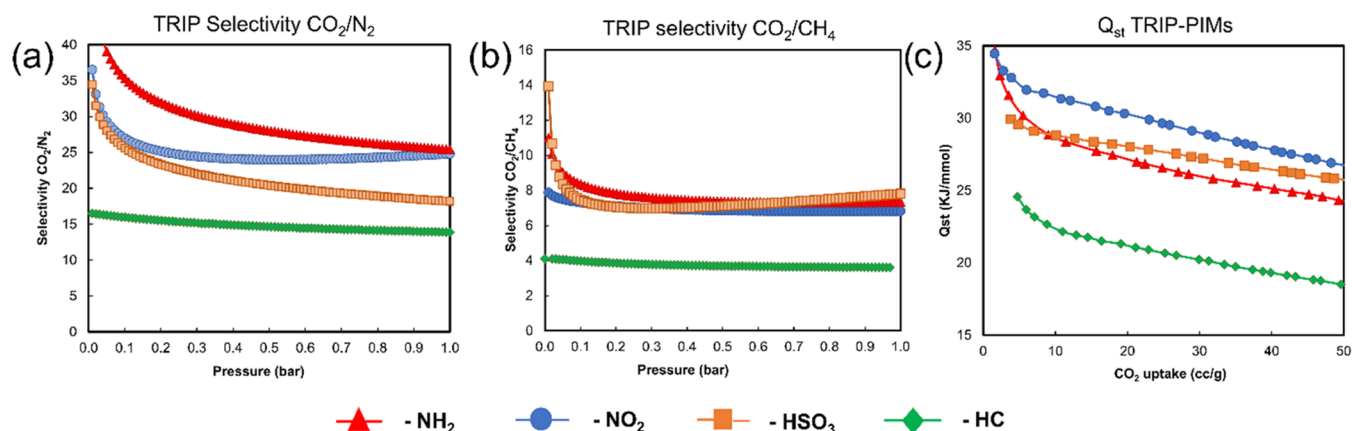


Figure 6. (a) IAST CO₂/N₂ selectivity (simulating a 15/85 composition), (b) IAST CO₂/CH₄ selectivity (simulating 50/50 composition), and (c) Q_{st} of TRIP-PIMs.

selectivity values are typically lower than the corresponding CO₂/N₂ for these kinds of porous polymers,^{61,62} yet the results obtained with our hyper-cross-linked PIMs proved competitive with state-of-the-art porous materials also for this separation, as shown in Table 1 and in Figure 6b. Even in this case, the best results were achieved with the aminated PIMs, with PIM-TPB-NH₂ that reached a CO₂/CH₄ selectivity of 8.6. The nitrated polymers proved to be almost as good as the aminated ones and so did the sulfonated ones. The enhanced selectivity of the substituted polymers could be also explained by analyzing their isosteric heats of adsorption, especially for the aminated and nitrated PIMs (Q_{st} in Table 1). In fact, the Q_{st} values obtained for these polymers show that their adsorption mechanism fits in between physisorption and chemisorption, although we believe that the values reflect that physisorption is the dominant mechanism, as the highest value (34.7 KJ mol⁻¹ for PIM-Trip-NH₂) approaches 50 KJ mol⁻¹ that is considered as the threshold between the two mechanisms.¹²

As discussed earlier, having a good compromise between physisorption and chemisorption is ideal, as a reasonable Q_{st} guarantees good affinity for CO₂, which improves its separation from other gases. At the same time, staying below 50 KJ mol⁻¹ ensures that the energy penalty of its desorption would not be very high.^{12,63} Figure 6c shows an example of the selectivity and the Q_{st} plots for the TRIP-PIM family; the single plots for all of the other polymers are reported in Figure S11.

CONCLUSIONS

The synthesis and characterization of a series of hyper-cross-linked PIMs prepared via a knitting method promoted by Friedel–Crafts polymerization provided interesting materials for CO₂ adsorption and selectivity toward N₂ and CH₄. The hydrocarbon-based polymers were functionalized postpolymerization to introduce polar groups, which helped us to tune the porosity and the polarity of the backbone, which produced an improvement of the CO₂ uptakes and the CO₂/N₂ and CO₂/CH₄ selectivity on the final materials. The data showed that the sulfonation of the hydrocarbon PIMs provided the best results in terms of CO₂ uptakes and CO₂/CH₄ selectivity, whereas the nitrated and aminated PIMs showed enhanced CO₂/N₂ selectivity. The new polymers proved to be competitive with state-of-the-art materials, and we believe that this is due to a combination of pore size, functionalization, and isosteric heats of adsorption, which makes them very attractive materials for

carbon capture and biogas upgrading applications. The ease of functionalization demonstrates that we can “play” with chemistry to tune the selectivity of these materials for the chosen gases. Finally, the isosteric heats of adsorption analysis suggests an adsorption mechanism in between physisorption and chemisorption, which is ideal for VSA as it assures a good affinity for CO₂ and a reduced energy penalty of its release.

ASSOCIATED CONTENT

Supporting Information

The Supporting Information is available free of charge at <https://pubs.acs.org/doi/10.1021/acsami.2c02604>.

Synthesis and characterization of polymers, selectivity CO₂/N₂ and CO₂/CH₄, isotherms, heats of adsorption, FTIR spectra, and solid-state ¹³C NMR spectra (PDF)

AUTHOR INFORMATION

Corresponding Author

Mariolino Carta – Department of Chemistry, Swansea University, College of Science, Swansea SA2 8PP, U.K.;
 orcid.org/0000-0003-0718-6971;
 Email: mariolino.carta@swansea.ac.uk

Authors

Haoli Zhou – Department of Chemistry, Swansea University, College of Science, Swansea SA2 8PP, U.K.; State Key Laboratory of Materials-Oriented Chemical Engineering, College of Chemical Engineering, Nanjing Tech University, Nanjing 210009, P. R. China; orcid.org/0000-0003-4699-5325

Christopher Rayer – Department of Chemistry, Swansea University, College of Science, Swansea SA2 8PP, U.K.

Ariana R. Antonangelo – Department of Chemistry, Swansea University, College of Science, Swansea SA2 8PP, U.K.

Natasha Hawkins – Department of Chemistry, Swansea University, College of Science, Swansea SA2 8PP, U.K.

Complete contact information is available at: <https://pubs.acs.org/10.1021/acsami.2c02604>

Author Contributions

H.Z., C.R., A.R.A., and N.H. carried out the synthesis and characterization of the polymers. M.C. designed the project and drafted the paper. All authors contributed to the writing of the paper and gave final approval for publication.

Notes

The authors declare no competing financial interest.

ACKNOWLEDGMENTS

Dr. Mariolino Carta, Dr. Ariana Antonangelo, and Natasha Hawkins gratefully acknowledge funding from the Engineering and Physical Sciences Research Council (EPSRC), Grant number: EP/T007362/1 “Novel polymers of intrinsic microporosity for heterogeneous base-catalyzed reactions (HBC-PIMs)” and Swansea University. Dr. Haoli Zhou gratefully acknowledges the Chinese scholarship number: CSC No. 201908320208 for his staying at Swansea University. The authors kindly acknowledge Daniel M. Dawson and the University of St. Andrews for the ^{13}C SSNMR service.

REFERENCES

- (1) Lielieveld, J.; Klingmüller, K.; Pozzer, A.; Burnett, R. T.; Haines, A.; Ramanathan, V. Effects of fossil fuel and total anthropogenic emission removal on public health and climate. *Proc. Natl. Acad. Sci. U.S.A.* **2019**, *116*, 7192.
- (2) NASA <https://climate.nasa.gov/vital-signs/carbon-dioxide/>.
- (3) Cook, J.; Oreskes, N.; Doran, P. T.; Anderegg, W. R. L.; Verheggen, B.; Maibach, E. W.; Carlton, J. S.; Lewandowsky, S.; Skuce, A. G.; Green, S. A.; Nuccitelli, D.; Jacobs, P.; Richardson, M.; Winkler, B.; Painting, R.; Rice, K. Consensus on consensus: a synthesis of consensus estimates on human-caused global warming. *Environ. Res. Lett.* **2016**, *11*, No. 048002.
- (4) Rogelj, J.; Shindell, D.; Jiang, K.; Fifita, S.; Forster, P.; Ginzburg, V.; Handa, C.; Khesghi, H.; Kobayashi, S.; Kriegler, E. Mitigation Pathways Compatible with 1.5 °C in the Context of Sustainable Development. In *Global Warming of 1.5 °C*, Intergovernmental Panel on Climate Change, 2018; pp 93–174.
- (5) Fuhrman, J.; Clarens, A.; Calvin, K.; Doney, S. C.; Edmonds, J. A.; O'Rourke, P.; Patel, P.; Pradhan, S.; Shobe, W.; McJeon, H. The role of direct air capture and negative emissions technologies in the shared socioeconomic pathways towards +1.5 °C and +2 °C futures. *Environ. Res. Lett.* **2021**, *16*, No. 114012.
- (6) Terlouw, T.; Treyer, K.; Bauer, C.; Mazzotti, M. Life Cycle Assessment of Direct Air Carbon Capture and Storage with Low-Carbon Energy Sources. *Environ. Sci. Technol.* **2021**, *55*, 11397–11411.
- (7) Shi, X.; Xiao, H.; Azarabadi, H.; Song, J.; Wu, X.; Chen, X.; Lackner, K. S. Sorbents for the direct capture of CO₂ from ambient air. *Angew. Chem., Int. Ed.* **2020**, *59*, 6984–7006.
- (8) Chen, L.; Deng, S.; Zhao, R.; Zhu, Y.; Zhao, L.; Li, S. Temperature swing adsorption for CO₂ capture: Thermal design and management on adsorption bed with single-tube/three-tube internal heat exchanger. *Appl. Therm. Eng.* **2021**, *199*, No. 117538.
- (9) Zhou, Y.; Su, T.; Ma, G.; Ibrahim, A.-R.; Hu, X.; Wang, H.; Li, J. Tetra-*n*-heptyl ammonium tetrafluoroborate: Synthesis, phase equilibrium with CO₂ and pressure swing adsorption for carbon capture. *J. Supercrit. Fluids* **2017**, *120*, 304–309.
- (10) Leperi, K. T.; Snurr, R. Q.; You, F. Optimization of Two-Stage Pressure/Vacuum Swing Adsorption with Variable Dehydration Level for Postcombustion Carbon Capture. *Ind. Eng. Chem. Res.* **2016**, *55*, 3338–3350.
- (11) Subraveti, S. G.; Roussanaly, S.; Anantharaman, R.; Riboldi, L.; Rajendran, A. How much can novel solid sorbents reduce the cost of post-combustion CO₂ capture? A techno-economic investigation on the cost limits of pressure–vacuum swing adsorption. *Appl. Energy* **2022**, *306*, No. 117955.
- (12) House, K. Z.; Harvey, C. F.; Aziz, M. J.; Schrag, D. P. The energy penalty of post-combustion CO₂ capture & storage and its implications for retrofitting the U.S. installed base. *Energy Environ. Sci.* **2009**, *2*, 193–205.
- (13) Bruch, L. W. Theory of physisorption interactions. *Surf. Sci.* **1983**, *125*, 194–217.
- (14) Huber, F.; Berwanger, J.; Polesya, S.; Mankovsky, S.; Ebert, H.; Giessibl Franz, J. Chemical bond formation showing a transition from physisorption to chemisorption. *Science* **2019**, *366*, 235–238.
- (15) Patel, H. A.; Byun, J.; Yavuz, C. T. Carbon Dioxide Capture Adsorbents: Chemistry and Methods. *ChemSusChem* **2017**, *10*, 1303–1317.
- (16) Zheng, S.; Zeng, S.; Li, Y.; Bai, L.; Bai, Y.; Zhang, X.; Liang, X.; Zhang, S. State of the art of ionic liquid-modified adsorbents for CO₂ capture and separation. *AIChE J.* **68**, e17500. DOI: 10.1002/aic.17500.
- (17) Kinik, F. P.; Uzun, A.; Keskin, S. Ionic Liquid/Metal–Organic Framework Composites: From Synthesis to Applications. *ChemSusChem* **2017**, *10*, 2842–2863.
- (18) Dai, Z.; Bao, Y.; Yuan, J.; Yao, J.; Xiong, Y. Different functional groups modified porous organic polymers used for low concentration CO₂ fixation. *Chem. Commun.* **2021**, *57*, 9732–9735.
- (19) Zhang, M.; Yu, A.; Wu, X.; Shao, P.; Huang, X.; Ma, D.; Han, X.; Xie, J.; Feng, X.; Wang, B. Sealing functional ionic liquids in conjugated microporous polymer membrane by solvent-assisted micropore tightening. *Nano Res.* **2021**, *15*, 2552–2557.
- (20) Eftaiha, A. F.; Qaroush, A. K.; Hasan, A. K.; Assaf, K. I.; Al-Qaisi, F. a.M.; Melhem, M. E.; Al-Maythalyon, B. A.; Usman, M. Cross-linked, porous imidazolium-based poly(ionic liquid)s for CO₂ capture and utilisation. *New J. Chem.* **2021**, *45*, 16452–16460.
- (21) McDonald, T. M.; Mason, J. A.; Kong, X.; Bloch, E. D.; Gygi, D.; Dani, A.; Crocellà, V.; Giordanino, F.; Odoh, S. O.; Drisdell, W. S.; Vlaisavljevich, B.; Dzubak, A. L.; Poloni, R.; Schnell, S. K.; Planas, N.; Lee, K.; Pascal, T.; Wan, L. F.; Prendergast, D.; Neaton, J. B.; Smit, B.; Kortright, J. B.; Gagliardi, L.; Bordiga, S.; Reimer, J. A.; Long, J. R. Cooperative insertion of CO₂ in diamine-appended metal-organic frameworks. *Nature* **2015**, *519*, 303–308.
- (22) Shao, L.; Liu, N.; Wang, L.; Sang, Y.; Zhan, P.; Zhang, L.; Huang, J.; Chen, J.; et al. Facile preparation of oxygen-rich porous polymer microspheres from lignin-derived phenols for selective CO₂ adsorption and iodine vapor capture. *Chemosphere* **2022**, *288*, No. 132499.
- (23) Ansari, M.; Hassan, A.; Alam, A.; Das, N. A mesoporous polymer bearing 3D-Triptycene, –OH and azo- functionalities: Reversible and efficient capture of carbon dioxide and iodine vapor. *Microporous Mesoporous Mater.* **2021**, *323*, No. 111242.
- (24) Najafi, P.; Ramezani-pour Penchah, H.; Ghaemi, A. Synthesis and characterization of Benzyl chloride-based hypercrosslinked polymers and its amine-modification as an adsorbent for CO₂ capture. *Environ. Technol. Innovation* **2021**, *23*, No. 101746.
- (25) Rong, M.; Yang, L.; Yang, C.; Yu, J.; Liu, H. Tetraphenyladamantane-based microporous polyaminals for efficient adsorption of CO₂, H₂ and organic vapors. *Microporous Mesoporous Mater.* **2021**, *323*, No. 111206.
- (26) Chen, J.; Li, H.; Zhong, M.; Yang, Q. Tuning the Surface Polarity of Microporous Organic Polymers for CO₂ Capture. *Chem. - Asian J.* **2017**, *12*, 2291–2298.
- (27) Shen, C.; Wang, Z. Tetraphenyladamantane-Based Microporous Polyimide and Its Nitro-Functionalization for Highly Efficient CO₂ Capture. *J. Phys. Chem. C* **2014**, *118*, 17585–17593.
- (28) Guo, Z.; Qu, Z.; Wu, H.; Zhao, R.; Wu, Y.; Liu, Y.; Yang, L.; Ren, Y.; Ye, C.; Jiang, Z. Polymer Electrolyte Membranes with Hybrid Cluster Network for Efficient CO₂/CH₄ Separation. *ACS Sustainable Chem. Eng.* **2020**, *8*, 6815–6825.
- (29) Lu, W.; Yuan, D.; Sculley, J.; Zhao, D.; Krishna, R.; Zhou, H.-C. Sulfonate-Grafted Porous Polymer Networks for Preferential CO₂ Adsorption at Low Pressure. *J. Am. Chem. Soc.* **2011**, *133*, 18126–18129.
- (30) McKeown, N. B. The synthesis of polymers of intrinsic microporosity (PIMs). *Sci. China: Chem.* **2017**, *60*, 1023–1032.
- (31) Carta, M.; Malpass-Evans, R.; Croad, M.; Rogan, Y.; Jansen, J. C.; Bernardo, P.; Bazzarelli, F.; McKeown, N. B. An efficient polymer molecular sieve for membrane gas separations. *Science* **2013**, *339*, 303–307.

- (32) Comesaña-Gándara, B.; Chen, J.; Bezzu, C. G.; Carta, M.; Rose, I.; Ferrari, M.-C.; Esposito, E.; Fuoco, A.; Jansen, J. C.; McKeown, N. B. Redefining the Robeson upper bounds for CO₂/CH₄ and CO₂/N₂ separations using a series of ultrapermeable benzotriptycene-based polymers of intrinsic microporosity. *Energy Environ. Sci.* **2019**, *12*, 2733–2740.
- (33) Wang, Y.; Ghanem, B. S.; Ali, Z.; Hazazi, K.; Han, Y.; Pinnau, I. Recent Progress on Polymers of Intrinsic Microporosity and Thermally Modified Analogue Materials for Membrane-Based Fluid Separations. *Small Struct.* **2021**, *2*, No. 2100049.
- (34) Lau, C. H.; Konstas, K.; Doherty, C. M.; Smith, S. J.; Hou, R.; Wang, H.; Carta, M.; Yoon, H.; Park, J.; Freeman, B. D.; et al. Tailoring molecular interactions between microporous polymers in high performance mixed matrix membranes for gas separations. *Nanoscale* **2020**, *12*, 17405–17410.
- (35) D'Alessandro, D. M.; Smit, B.; Long, J. R. Carbon Dioxide Capture: Prospects for New Materials. *Angew. Chem., Int. Ed.* **2010**, *49*, 6058–6082.
- (36) Jue, M. L.; Lively, R. P. PIM hybrids and derivatives: how to make a good thing better. *Curr. Opin. Chem. Eng.* **2022**, *35*, No. 100750.
- (37) Msayib, K. J.; McKeown, N. B. Inexpensive polyphenylene network polymers with enhanced microporosity. *J. Mater. Chem. A* **2016**, *4*, 10110–10113.
- (38) Lau, C. H.; Lu, T.-d.; Sun, S.-P.; Chen, X.; Carta, M.; Dawson, D. M. Continuous flow knitting of a triptycene hypercrosslinked polymer. *Chem. Commun.* **2019**, *55*, 8571–8574.
- (39) Al-Hetlani, E.; Amin, M. O.; Antonangelo, A. R.; Zhou, H.; Carta, M. Triptycene and triphenylbenzene-based polymers of intrinsic microporosity (PIMs) for the removal of pharmaceutical residues from wastewater. *Microporous Mesoporous Mater.* **2022**, *330*, No. 111602.
- (40) Stavropoulos, G. G.; Samaras, P.; Sakellariopoulos, G. P. Effect of activated carbons modification on porosity, surface structure and phenol adsorption. *J. Hazard. Mater.* **2008**, *151*, 414–421.
- (41) Liu, Y.; Wu, S.; Wang, G.; Yu, G.; Guan, J.; Pan, C.; Wang, Z. Control of porosity of novel carbazole-modified polytriazine frameworks for highly selective separation of CO₂–N₂. *J. Mater. Chem. A* **2014**, *2*, 7795–7801.
- (42) Xing, W.; Liu, C.; Zhou, Z.; Zhang, L.; Zhou, J.; Zhuo, S.; Yan, Z.; Gao, H.; Wang, G.; Qiao, S. Z. Superior CO₂ uptake of N-doped activated carbon through hydrogen-bonding interaction. *Energy Environ. Sci.* **2012**, *5*, 7323–7327.
- (43) Mahurin, S. M.; Górka, J.; Nelson, K. M.; Mayes, R. T.; Dai, S. Enhanced CO₂/N₂ selectivity in amidoxime-modified porous carbon. *Carbon* **2014**, *67*, 457–464.
- (44) Islamoglu, T.; Kim, T.; Kahveci, Z.; El-Kadri, O. M.; El-Kaderi, H. M. Systematic Postsynthetic Modification of Nanoporous Organic Frameworks for Enhanced CO₂ Capture from Flue Gas and Landfill Gas. *J. Phys. Chem. C* **2016**, *120*, 2592–2599.
- (45) Salarizadeh, P.; Javanbakht, M.; Pourmahdian, S.; Hazer, M. S. A.; Hooshyari, K.; Askari, M. B. Novel proton exchange membranes based on proton conductive sulfonated PAMPS/PSSA-TiO₂ hybrid nanoparticles and sulfonated poly (ether ether ketone) for PEMFC. *Int. J. Hydrogen Energy* **2019**, *44*, 3099–3114.
- (46) Huh, S.; Chen, H. T.; Wiench, J. W.; Pruski, M.; Lin, V. S. Y. Cooperative catalysis by general acid and base bifunctionalized mesoporous silica nanospheres. *Angew. Chem.* **2005**, *117*, 1860–1864.
- (47) Carta, M.; Msayib, K. J.; Budd, P. M.; McKeown, N. B. Novel spirobisindanes for use as precursors to polymers of intrinsic microporosity. *Org. Lett.* **2008**, *10*, 2641–2643.
- (48) Alahmed, A. H.; Briggs, M. E.; Cooper, A. I.; Adams, D. J. Postsynthetic fluorination of Scholl-coupled microporous polymers for increased CO₂ uptake and selectivity. *J. Mater. Chem. A* **2019**, *7*, 549–557.
- (49) Rozyyev, V.; Hong, Y.; Yavuz, M. S.; Thirion, D.; Yavuz, C. T. Extensive Screening of Solvent-Linked Porous Polymers through Friedel–Crafts Reaction for Gas Adsorption. *Adv. Energy Sustainability Res.* **2021**, *2*, No. 2100064.
- (50) He, Y.; Zhu, X.; Li, Y.; Peng, C.; Hu, J.; Liu, H. Efficient CO₂ capture by triptycene-based microporous organic polymer with functionalized modification. *Microporous Mesoporous Mater.* **2015**, *214*, 181–187.
- (51) Thommes, M.; Kaneko, K.; Neimark, A. V.; Olivier, J. P.; Rodriguez-Reinoso, F.; Rouquerol, J.; Sing, K. S. Physisorption of gases, with special reference to the evaluation of surface area and pore size distribution (IUPAC Technical Report). *Pure Appl. Chem.* **2015**, *87*, 1051–1069.
- (52) Lozano-Castelló, D.; Cazorla-Amorós, D.; Linares-Solano, A. Usefulness of CO₂ adsorption at 273 K for the characterization of porous carbons. *Carbon* **2004**, *42*, 1233–1242.
- (53) Liu, Y.; Wang, S.; Meng, X.; Ye, Y.; Song, X.; Liang, Z. Increasing the surface area and CO₂ uptake of conjugated microporous polymers via a post-knitting method. *Mater. Chem. Front.* **2021**, *5*, 5319–5327.
- (54) Lin, R.-B.; He, Y.; Li, P.; Wang, H.; Zhou, W.; Chen, B. Multifunctional porous hydrogen-bonded organic framework materials. *Chem. Soc. Rev.* **2019**, *48*, 1362–1389.
- (55) Tan, H.; Chen, Q.; Chen, T.; Wei, Z.; Liu, H. CO₂/CH₄ separation using flexible microporous organic polymers with expansion/shrinkage transformations during adsorption/desorption processes. *Chem. Eng. J.* **2020**, *391*, No. 123521.
- (56) Saleh, M.; Lee, H. M.; Kemp, K. C.; Kim, K. S. Highly Stable CO₂/N₂ and CO₂/CH₄ Selectivity in Hyper-Cross-Linked Heterocyclic Porous Polymers. *ACS Appl. Mater. Interfaces* **2014**, *6*, 7325–7333.
- (57) Fayemiwo, K. A.; Vladislavljević, G. T.; Nabavi, S. A.; Benyahia, B.; Hanak, D. P.; Loponov, K. N.; Manović, V. Nitrogen-rich hypercrosslinked polymers for low-pressure CO₂ capture. *Chem. Eng. J.* **2018**, *334*, 2004–2013.
- (58) Ntiamoah, A.; Ling, J.; Xiao, P.; Webley, P. A.; Zhai, Y. CO₂ capture by vacuum swing adsorption: role of multiple pressure equalization steps. *Adsorption* **2015**, *21*, 509–522.
- (59) Myers, A. L.; Prausnitz, J. M. Thermodynamics of mixed-gas adsorption. *AIChE J.* **1965**, *11*, 121–127.
- (60) Lee, S.; Lee, J. H.; Kim, J. User-friendly graphical user interface software for ideal adsorbed solution theory calculations. *Korean J. Chem. Eng.* **2018**, *35*, 214–221.
- (61) Lv, D.; Chen, J.; Yang, K.; Wu, H.; Chen, Y.; Duan, C.; Wu, Y.; Xiao, J.; Xi, H.; Li, Z.; Xia, Q. Ultrahigh CO₂/CH₄ and CO₂/N₂ adsorption selectivities on a cost-effectively L-aspartic acid based metal-organic framework. *Chem. Eng. J.* **2019**, *375*, No. 122074.
- (62) Park, J.; Attia, N. F.; Jung, M.; Lee, M. E.; Lee, K.; Chung, J.; Oh, H. Sustainable nanoporous carbon for CO₂, CH₄, N₂, H₂ adsorption and CO₂/CH₄ and CO₂/N₂ separation. *Energy* **2018**, *158*, 9–16.
- (63) Wu, X.; Yu, Y.; Qin, Z.; Zhang, Z. The Advances of Post-combustion CO₂ Capture with Chemical Solvents: Review and Guidelines. *Energy Procedia* **2014**, *63*, 1339–1346.
- (64) Cucu, E.; Dalkılıç, E.; Altundas, R.; Sadak, A. E. Gas sorption and selectivity study of N,N,N',N'-tetraphenyl-1,4-phenylenediamine based microporous hyper-crosslinked polymers. *Microporous Mesoporous Mater.* **2022**, *330*, No. 111567.
- (65) Sadak, A. E.; Karakuş, E.; Chumakov, Y. M.; Dogan, N. A.; Yavuz, C. T. Triazatruxene-Based Ordered Porous Polymer: High Capacity CO₂, CH₄, and H₂ Capture, Heterogeneous Suzuki–Miyaura Catalytic Coupling, and Thermoelectric Properties. *ACS Appl. Energy Mater.* **2020**, *3*, 4983–4994.
- (66) Shao, L.; Wang, S.; Liu, M.; Huang, J.; Liu, Y.-N. Triazine-based hyper-cross-linked polymers derived porous carbons for CO₂ capture. *Chem. Eng. J.* **2018**, *339*, 509–518.
- (67) Shao, L.; Sang, Y.; Huang, J.; Liu, Y.-N. Triazine-based hyper-cross-linked polymers with inorganic-organic hybrid framework derived porous carbons for CO₂ capture. *Chem. Eng. J.* **2018**, *353*, 1–14.
- (68) Hong, L.; Ju, S.; Liu, X.; Zhuang, Q.; Zhan, G.; Yu, X. Highly Selective CO₂ Uptake in Novel Fishnet-like Polybenzoxazine-Based Porous Carbon. *Energy Fuels* **2019**, *33*, 11454–11464.

(69) Hou, S.; Tan, B. Naphthyl Substitution-Induced Fine Tuning of Porosity and Gas Uptake Capacity in Microporous Hyper-Cross-Linked Amine Polymers. *Macromolecules* **2018**, *51*, 2923–2931.

(70) Liu, G.; Wang, Y.; Shen, C.; Ju, Z.; Yuan, D. A facile synthesis of microporous organic polymers for efficient gas storage and separation. *J. Mater. Chem. A* **2015**, *3*, 3051–3058.